# Amino Acid-Dependent Attenuation of Toll-like Receptor Signaling by Peptide-Gold Nanoparticle Hybrids

**Hong Yang,[*,†] Shan-Yu Fung,[†] Shuyun Xu,[‡] Darren P. Sutherland,[†] Tobias R. Kollmann,[†] Mingyao Liu,[*,§,‡] and Stuart E. Turvey[*,§,†]**

[†]BC Children's Hospital and Child & Family Research Institute; Department of Pediatrics, Faculty of Medicine, University of British Columbia, Vancouver, British Columbia V5Z 4H4, Canada and [‡]Latner Thoracic Surgery Research Laboratories, Toronto General Research Institute, University Health Network; Department of Surgery, Faculty of Medicine, University of Toronto, Toronto, Ontario M5G 1L7, Canada. [§]M.L. and S.E.T contributed equally to the paper as senior authors.

**ABSTRACT** Manipulation of immune responsiveness using nanodevices provides a potential approach to treat human diseases. Toll-like receptor (TLR) signaling plays a central role in the pathophysiology of many acute and chronic human inflammatory diseases, and pharmacological regulation of TLR responses is anticipated to be beneficial in many of these inflammatory conditions. Here we describe the discovery of a unique class of peptide-gold nanoparticle hybrids that exhibit a broad inhibitory activity on TLR signaling, inhibiting signaling through TLRs 2, 3, 4, and 5. As exemplified using TLR4, the nanoparticles were found to inhibit both arms of TLR4 signaling cascade triggered by the prototypical ligand, lipopolysaccharide (LPS). Through structure—activity relationship studies, we identified the key chemical components of the hybrids that contribute to their immunomodulatory activity. Specifically, the hydrophobicity and aromatic ring structure of the amino acids on the peptides were essential for modulating TLR4 responses. This work enhances our fundamental understanding of the role of nanoparticle surface chemistry in regulating innate immune signaling, and identifies specific nanoparticle hybrids that may represent a unique class of anti-inflammatory therapeutics for human inflammatory diseases.

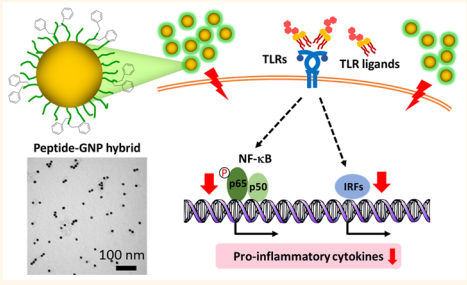


**KEYWORDS:** gold nanoparticles · peptides · Toll-like receptor signaling · immune modulation · surface chemistry · amino acids · NF-κB · IRF3

The innate immune system is a fundamental and ancient host defense mechanism critical for recognizing pathogens and empowering protective immune responses. Understanding of innate immunity was accelerated in the mid-1990s when the *Drosophila melanogaster* protein, Toll, was shown to be critical for defending fruit flies against infections.[1] This opened up a new avenue of research characterizing similar proteins, called Toll-like receptors (TLRs), in mammalian cells. Functional analysis of TLRs has revealed that they recognize and respond to variety of specific microbial molecules—pathogen-associated molecular patterns (PAMPs)—which are conserved among pathogens. These molecular "signatures" enable the innate immune system to discriminate among groups of pathogens and to induce an appropriate cascade of effector responses. Collectively, the complete TLR family allows the host to detect infection with most types of pathogens.[2,3]

Among the TLR family, TLR4 has been the most widely studied and has unique features in its downstream signaling pathways. TLR4 recognizes lipopolysaccharide (LPS), a component of the bacterial cell wall, and triggers two parallel signaling cascades: (a) the myeloid differentiation primary response gene 88 (MyD88)-dependent pathway uses the adapter molecule MyD88 leading to early activation of the transcription factors, NF-κB and AP-1, and production of pro-inflammatory cytokines; (b) the MyD88-independent pathway signals through TIR-domain-containing adapter inducing interferon-beta (TRIF) leading to activation of interferon regulatory factor 3 (IRF3) together with late-phase activation of NF-κB driving secretion of IFN-β and other cytokines.[4] All other TLRs (except TLR3, which signals exclusively through the

* Address correspondence to hyang@cfri.ca, mingyao.liu@utoronto.ca, sturvey@cw.bc.ca.

Received for review October 2, 2014 and accepted June 17, 2015.

**Published online June 17, 2015**
**10.1021/nn505634h**

MyD88-independent pathway) engage the MyD88-dependent signaling cascade.

TLR signaling can be viewed as a "double-edged sword". Despite its vital role in host defense against infections, vigorous innate immune responses generated by TLR activation can also be harmful. Indeed, such harmful TLR responses contribute to pathology in many human diseases. For example, acute excessive TLR4 activation has been associated with high morbidity during sepsis.[5,6] In addition, TLR responses (including TLR4) are pathologically relevant in diseases of food-producing animals (*e.g.*, bovine mastitis, the most common and costly disease of dairy cattle worldwide).[7,8] Therefore, attenuating TLR signaling has emerged as a novel therapeutic strategy for many inflammatory diseases.

Nanotechnology offers new powerful tools to manipulate immune responsiveness in the treatment of human diseases. Nanodevices can be rationally designed to tailor functionality for a specific application. For example, nanoparticles can be designed to either boost antigen specific immune responses for vaccine development,[9,10] or alternatively, to suppress immune responses to reduce transplant rejection and to treat inflammatory diseases.[11−14] Nanoparticles can also optimize therapeutic outcomes by improving *in vivo* biodistribution, achieving tissue/cell targeting, and sustaining the release of drugs.[15−17] Importantly, nanoparticles have been found to preferentially target phagocytic innate immune cells,[18,19] which makes them a compelling new generation of therapeutic agents to modulate inflammatory responses in specific tissues/organs.

In seeking nanoparticles that potently inhibit TLR signaling, we screened a library of physiologically stable peptide-gold nanoparticle hybrids developed through our previous studies.[20,21] These nanoparticle hybrids have tunable surface chemistry (achieved by altering the peptide ligands) and can serve as a model system allowing us to study whether nanodevice chemistry influences TLR signaling. We focused on TLR4 signaling (triggered by the canonical ligand, LPS) for initial screening as it utilizes both the MyD88-dependent and MyD88-independent signaling pathways, thus encompasses a wide range of signaling pathways. With this unbiased approach, we identified a specific nanoparticle hybrid (designated P12) that potently inhibited both arms of TLR4 signaling pathway. We further established that hydrophobicity and the aromatic ring structure of the amino acids were the key chemical components in the nanoparticle hybrids that contribute to this inhibitory activity. We then expanded our investigation to other TLRs (2, 3 and 5) to evaluate the specificity of the nanoparticles in blocking TLR signaling, and found that P12 was indeed able to inhibit signaling through TLRs 2, 3, 4, and 5. This study has defined the chemistry of nanoparticle-mediated immune modulation, and has identified a novel class of nanoparticle hybrids with immunomodulatory potential.

## RESULTS

**Construction of the Peptide-Gold Nanoparticle Hybrid Library.** In order to identify nanoparticles that can modulate TLR signaling, we first screened a library of peptide-gold nanoparticle hybrids that were established in our previous studies.[20,21] The hybrids were made of a gold nanoparticle (GNP) core with a diameter of ~13 nm and modified with a peptide shell containing a single or binary mixture of the peptide ligands (Figure 1A). The goal of modifying the GNPs with the peptide ligands was to improve their physiological stability and to change the surface properties of the hybrids. The peptide sequences used in this study are listed in Supporting Information (Table S1). This library of nanoparticles has a number of unique design features. First, the nanoparticles share a similar size and the same type of surface charge (negative charge), and they are stable under physiological conditions (*e.g.*, phosphate buffered saline and culture media containing serum). Second, the surface chemistry of the hybrids is tunable by introducing a second peptide (up to 10% of the total peptides utilized) that has a different terminal amino acid (C-terminal, facing away from the nanoparticles). We engineered nanoparticles that can be classified into three groups based on surface chemistry: (1) hydrophilic; (2) hydrophobic (nonaromatic); and (3) aromatic ring structured. Third, the peptide ligand density can be tuned to further program and optimize the surface chemistry of the nanoparticles for specific applications. Although our library of the peptide-GNP hybrids is relatively small, it is deliberately designed to identify the key chemical features of the nanoparticles that play an important role in immune modulation.

**Screening Nanoparticle Hybrids for Modulators of TLR4 Signaling.** Among the TLR family, TLR4 signaling pathway is an informative pathway for screening as it utilizes both the MyD88-dependent and MyD88-independent (*via* TRIF) signaling cascades and thus captures both molecular pathways involved in TLR responsiveness (see Figure 1B for a schematic overview of the TLR4 signaling cascade).

The screening was conducted on two types of reporter cells engineered from human monocytic THP-1 cells. Cells were differentiated into macrophages to enhance the phagocytic capability, to boost the LPS-induced responses, and to mimic the native monocyte-derived macrophages. One reporter line stably expresses an NF-$\kappa$B/AP-1 responsive element and responds to LPS in a dose-dependent manner (Figure 1C). The second type of reporter cell line relies upon luciferase secretion under the control of interferon (IFN)-stimulated gene promoter and IFN-stimulated response elements.

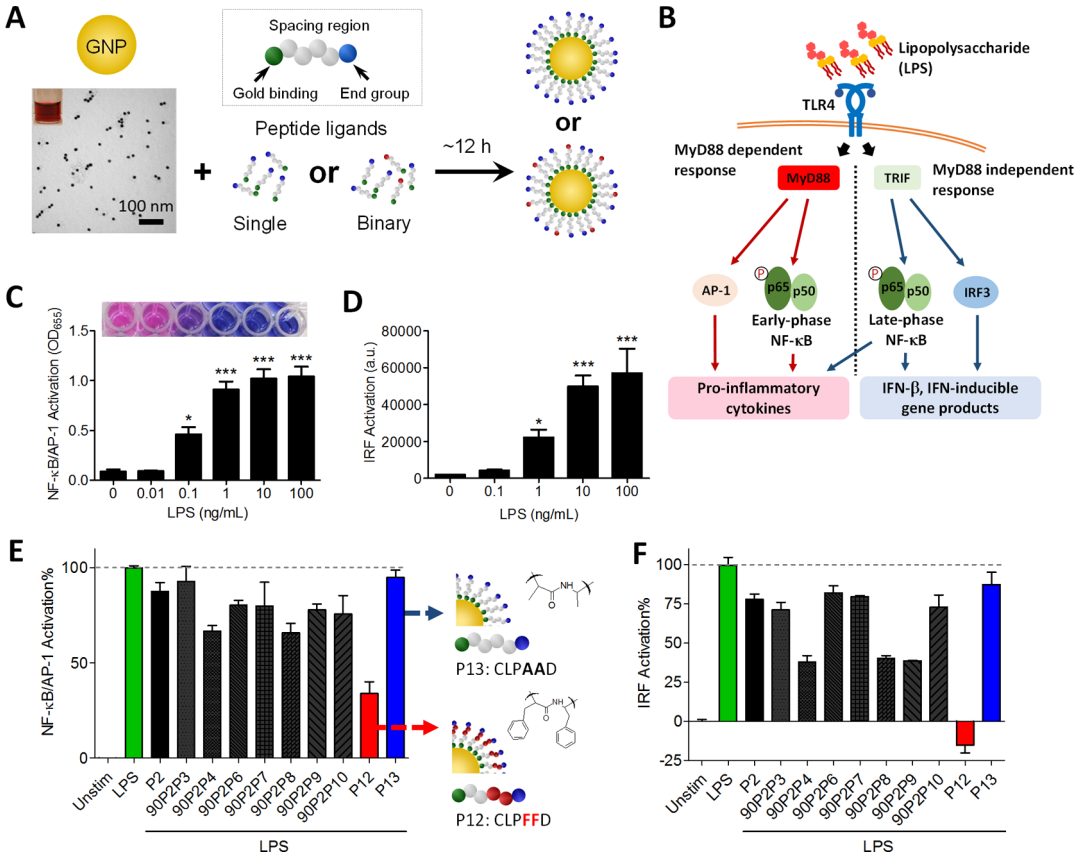


**Figure 1. Screening of nanoparticles for modulators of TLR4 signaling. (A) Establishment of the peptide-GNP hybrid library. (B) A simplified diagram of the two arms of TLR4 signaling pathway. (C) LPS dose response of NF-κB/AP-1 activation (inset shows color change in the wells). (D) LPS dose response of IRF activation. (E,F) Screening of nanoparticles modulators on THP-1 cell-derived macrophages with NF-κB/AP-1 (E) and IRF (F) reporter systems. Nanoparticle concentration = 100 nM.**

Upon LPS stimulation, IRF3 is activated by the MyD88-independent pathway (see Figure 1B), and Figure 1D shows the LPS dose responsiveness of IRF activation. Our screening approach allowed us to study the effects of nanoparticle treatment on both MyD88-dependent and -independent pathways following a single stimulation with LPS.

Altogether, ten nanoparticle hybrids were screened. Among them, one hybrid (P12) strongly inhibited both NF-κB/AP-1 (Figure 1E) and IRF3 activation (Figure 1F). Interestingly, the hybrid P13, which only differs from P12 by a change in the C-terminal peptide sequence from phenylalanine to alanine, displayed no inhibitory activity (Figure 1E,F). In addition, we found the hybrids exhibiting moderate inhibitory activity were composed of binary peptide ligand mixtures containing amino acids with aromatic structures (P4, P8 and P9). On the basis of the finding that the nanoparticle hybrid P12 could inhibit both arms of TLR4 signaling cascade, P12 became the lead nanoparticle for further validation and mechanistic studies, with the inactive single amino acid variant, P13, serving as a control.

**Validation of the Lead Nanoparticle Hybrid P12.** We first evaluated the effect of the hybrids P12 and P13 on both MyD88-dependent and -independent pathways triggered by various concentrations of LPS ranging from 1 ng/mL to 10 μg/mL (Figure 2A,B). We found that P12 and P13 did not significantly alter the baseline of NF-κB/AP-1 and IRF activation in the absence of LPS stimulation. However, in the presence of LPS (at all concentrations), P12 significantly reduced the LPS-induced NF-κB/AP-1 and IRF activation, while P13 did not. The inhibitory effect was not due to the cellular toxicity (Figure 2C). These observations confirmed that the hybrid P12 has potent inhibitory activity on both signaling cascades downstream of the TLR4.

We next evaluated whether the inhibitory effect originated from either the peptide ligands alone or the bare gold nanoparticles. Before LPS stimulation, the reporter cells were treated with either peptides alone (10 μM) or the gold nanoparticles capped with serum proteins from the culture medium (as the bare gold nanoparticles are not stable and aggregate at physiological salt concentrations). These control experiments revealed that neither the peptide ligands nor gold nanoparticles alone significantly impacted NF-κB/AP-1 and IRF activation (Figure 2D,E). These data demonstrated that the individual nonbioactive molecules can

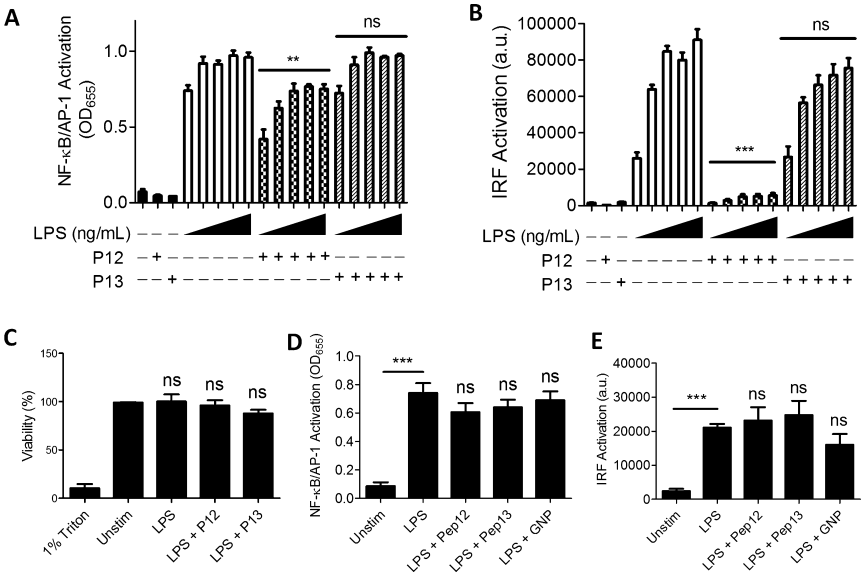


**Figure 2. Lead peptide-GNP hybrid P12 attenuates both arms of TLR4 signaling in THP-1 cell-derived macrophages. (A,B) Inhibition of NF-κB/AP-1 (A) and IRF (B) activation by P12 upon LPS stimulation (from 1 ng/mL to 10 μg/mL) in comparison with the inactive P13. (C) The LPS stimulation and nanoparticle treatments do not affect the cell viability. (D,E) Effects of the peptide ligands (10 μM) and gold nanoparticles (100 nM) alone on the LPS (1 ng/mL) induced NF-κB/AP-1 (D) and IRF (E) activation. $n = 3-4$, ns: not significant, *$p < 0.05$, ***$p < 0.001$ *vs* LPS at the same concentration.**

exhibit inhibitory biological function when assembled as a nanodevice.

To confirm the inhibitory activity of P12 using a complementary experimental approach, we measured NF-κB and IRF3 protein modifications *via* immunoblotting with densitometric quantification. Specifically, the activation of NF-κB was measured by both the phosphorylation of the NF-κB subunit, p65, and degradation of the inhibitory protein, IκBα, while IRF3 activation was monitored using IRF3 phosphorylation. As shown in Figure 3A,B, LPS stimulation (10 ng/mL) resulted in a time-dependent response of p65 phosphorylation, IκBα degradation, and IRF3 phosphorylation. The presence of P12 significantly inhibited and delayed p65 phosphorylation, IκBα degradation, and IRF3 phosphorylation (Figure 3A, C−E). In contrast, the inactive nanoparticle hybrid P13 had no impact on LPS induced NF-κB and IRF3 activation (Figure 3B−E). Collectively, these data confirmed that the lead nanoparticle, P12, directly interferes in signals leading to NF-κB and IRF3 molecular modifications downstream of TLR4.

**Effect of P12 on the Cytokine Production Profile.** Cytokine secretion is one of the major outcomes of intact TLR4 signaling. Therefore, we quantified the impact of P12 on LPS-driven cytokine secretion. As anticipated, secretion of a variety of cytokines were up-regulated by LPS stimulation (10 ng/mL) (indicated in red in Figure 4A). Treatment with the lead nanoparticle P12 reduced secretion of a number of cytokines, with the most significant reductions seen in MCP-1, IL-1α, GRO-α and MIP-1β. Again, the control nanoparticle P13 did not significantly alter the cytokine production profile compared with LPS-only stimulation. To validate the cytokine array results, we used enzyme-linked immunosorbent assay (ELISA) to measure selected cytokines (IL-6, MCP-1, GRO-α, and MIP-1β) at two time points following LPS exposure: 4 and 24 h. P12 reduced MCP-1, GRO-α, and MIP-1β levels close to the baseline, but not IL-6, when quantified at 24 h (Figure 4B−E). Cytokine production at 4 h had a similar pattern of inhibition (Supporting Information Figure S1). These observations demonstrated that the nanoparticle P12 has potent anti-inflammatory activity and can significantly reduce secretion of pro-inflammatory cytokines following LPS stimulation.

It is essential to evaluate whether the nanoparticle P12 demonstrates inhibitory activity on primary human immune cells. For this purpose, human peripheral blood mononuclear cells (PBMCs) were isolated from healthy volunteers. PBMCs contain a variety of immune cells including monocytes, lymphocytes, and dendritic cells. P12, but not P13, significantly inhibited secretion of MCP-1 and MIP-1β by fresh human PBMCs following stimulation with LPS (Figure 4F,G), confirming the potency of P12 in human primary immune cells.

**Structure/Chemistry−Activity Relationship Studies.** To elucidate the mechanisms responsible for P12 inhibition of the TLR4 signaling cascade from a materials chemistry perspective, we studied the relationship between the nanoparticle surface structure/chemistry and inhibitory activity. Comparing the two nanoparticle hybrids (P12 and P13), the only difference is that the peptide ligands on P12 contain two phenylalanine residues (FF), which are replaced with two alanine residues (AA) in P13 (Figure 1E). This difference suggests that the two adjacent phenylalanine residues

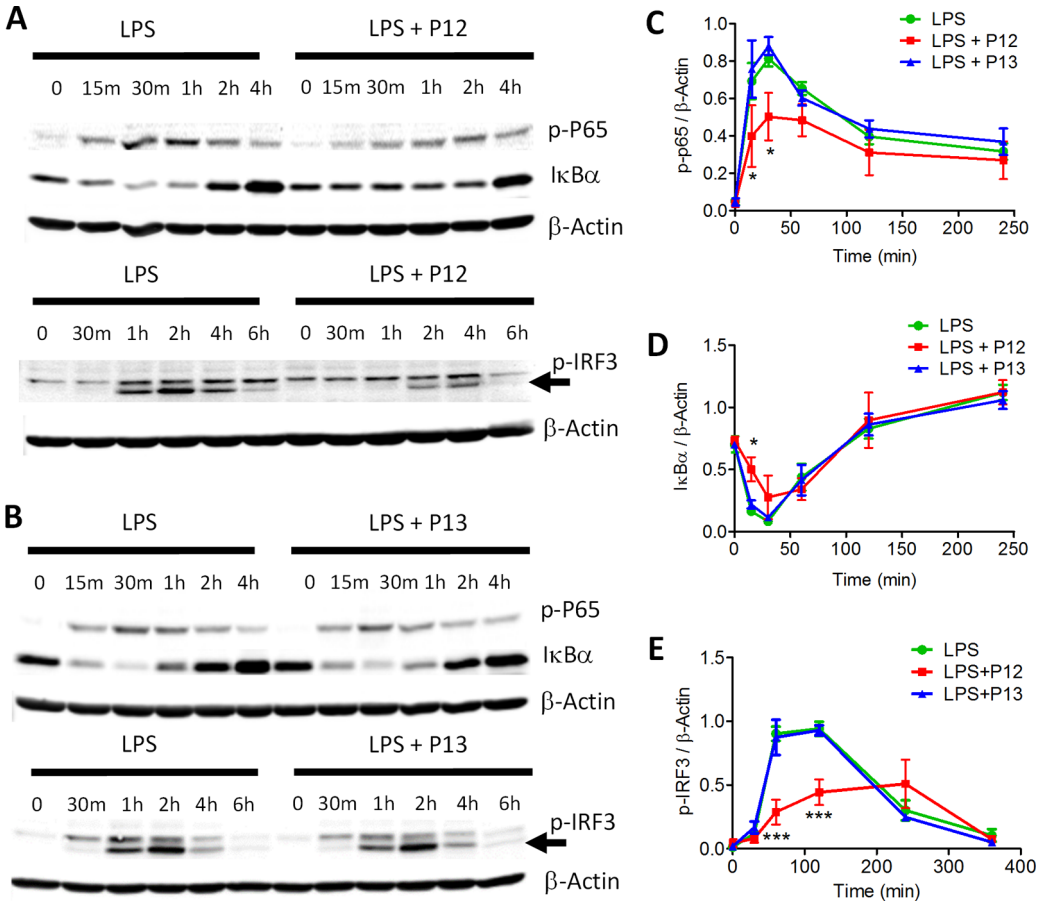


**Figure 3. Validation of the inhibitory activity of P12 by direct measurement of NF-κB (phosphorylation of p65 and IκBα degradation) and IRF3 (phosphorylation of IRF3, arrow indicated specific p-IRF3 band) signals on THP-1 cell-derived macrophages. (A) P12 treatment. (B) P13 treatment. (C–E) Densitometry analysis of p-p65 (C), IκBα (D) and p-IRF3 (E) from three independent measurements. LPS = 10 ng/mL, *$p < 0.05$, ***$p < 0.001$ *vs* LPS at the same time point.**

may play an important role in the anti-inflammatory activity of P12. To test this experimentally, we mutated each of the two phenylalanine residues to alanine (Figure 5A) and tested their immunomodulatory activity. We found that after changing either the inner (P14) or outer (P15) phenylalanine to alanine, the inhibitory effect on NF-κB/AP-1 activation was reduced. Nonetheless, change of the inner phenylalanine to alanine (P14) still exhibited a slight significant inhibitory effect on NF-κB/AP-1 activation (Figure 5B). In contrast, both P14 and P15 retained some IRF inhibitory activity, although this was more modest than P12 (Figure 5C). The inhibitory effect of P14 appeared to be stronger than P15. This trend was also true for MCP-1 and MIP-1$\beta$ cytokine production (Supporting Information Figure S2). These data suggested that the presence of phenylalanine on the surface of the hybrids contributes to the attenuation of TLR4 signaling with preferential inhibition toward the MyD88-independent pathway. In addition, our data revealed that the position of phenylalanine is important in determining inhibitory activity. Together, these observations supported our hypothesis that the two adjacent phenylalanine residues appear essential for the potent inhibitory activity of P12 on both arms of TLR4 signaling.

However, it remained unclear whether specific chemical features of phenylalanine (*i.e.*, hydrophobicity or the aromatic ring structure) were critical for the anti-inflammatory activity. To address this knowledge gap, we systematically mutated the two adjacent phenylalanine residues on P12 generating three distinct groups of hybrids: Group 1, hydrophobic, non-aromatic amino acids leucine (L) (P16), isoleucine (I) (P17) and valine (V) (P18); Group 2, aromatic ring bearing amino acids tyrosine (Y) (P19) and tryptophan (W) (P20); and Group 3, hydrophilic amino acids serine (S) (P21) and threonine (T) (P22) (Figure 6A). For the Group 1 alterations (addressing hydrophobicity), we found that P16 (FF → LL) and P17 (FF → II) significantly reduced NF-κB/AP-1 and IRF activation, but were less active than P12 (Figure 6B,C). P18 (FF → VV) showed only a slight inhibitory effect on TLR4 signaling. For Group 2 alterations (addressing aromatic structure), we found that both P19 (FF → YY) and P20 (FF → WW) retained significant inhibitory activity, with P20 displaying activity similar to P12 (Figure 6B,C). In contrast, the hydrophilic alterations (Group 3), P21 (FF → SS) and

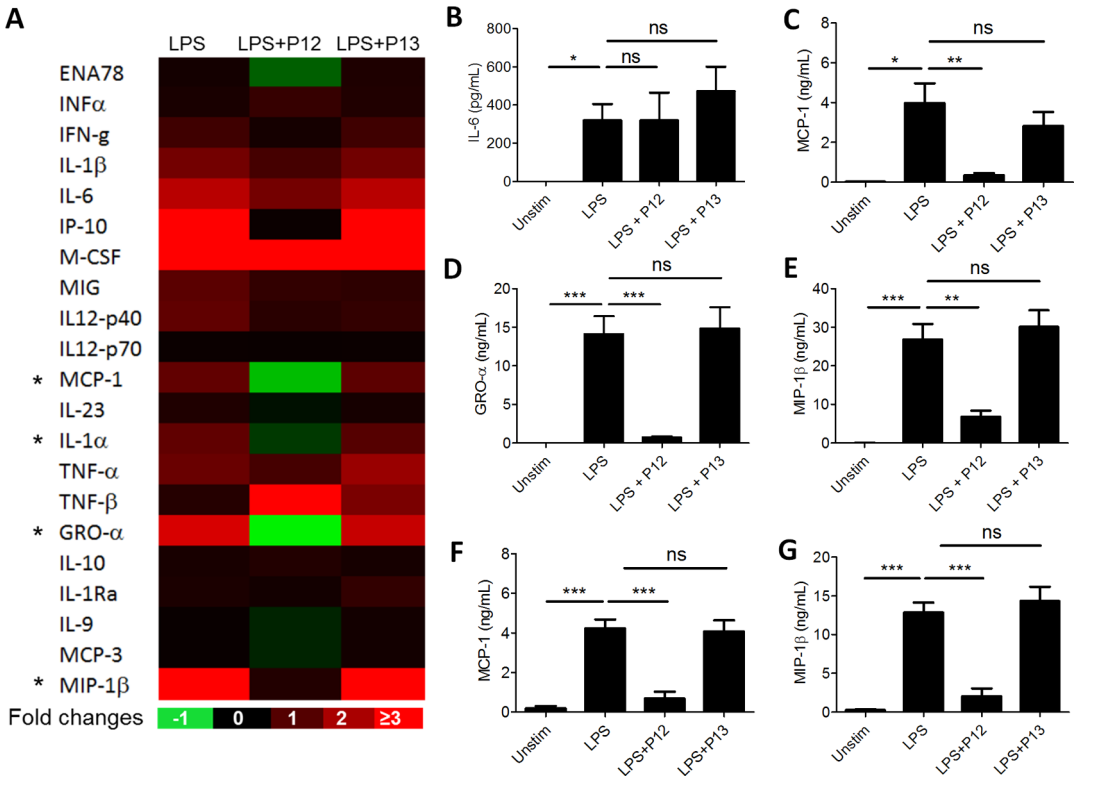


**Figure 4. Cytokine production profiles. (A) Multiplexed cytokine array profile of THP1-Dual cell-derived macrophages stimulated by LPS with or without P12 or P13 treatment. Different color codes represent the mean fold changes normalized to unstimulated sample, $n = 3$. (B–E) Selected cytokines, including IL-6 (B), MCP-1 (C), GRO-α (D) and MIP-1β (E) were validated by ELISA on supernatants from THP-1 cell-derived macrophages, $n = 4$. (F, G) Cytokine production by human PBMCs stimulated with LPS in the presence or absence of P12 and P13. Nanoparticle concentration =100 nM, LPS = 10 ng/mL, $n = 4$, ns: not significant, *$p < 0.05$, **$p < 0.01$, ***$p < 0.001$.**

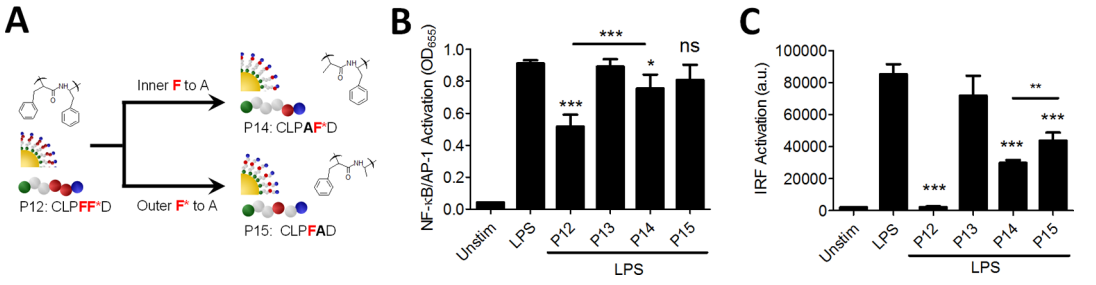


**Figure 5. Effect of the phenylalanine (F) residues of P12 on the TLR4 inhibitory activity. (A) A scheme showing the single mutation of the two phenylalanine residues (FF*) to alanine (A): inner F to A (P14) and outer F* to A (P15). (B,C) Inhibition of NF-κB/AP-1 (B) and IRF (C) activation upon LPS stimulation (10 ng/mL) by the mutated P14 and P15 in comparison with P12. ns: not significant, *$p < 0.05$, **$p < 0.01$, ***$p < 0.001$ *vs* LPS unless otherwise indicated, $n = 4$.**

P22 (FF → TT) displayed no inhibitory activity (Figure 6B,C). This was confirmed by measuring their impact on MCP-1 and MIP-1β production (Figure 6D,E). Together, our results suggested that both amino acid hydrophobicity and their aromatic ring structure play a critical role in inhibiting TLR4 signaling.

To generalize the relationship between the amino acid hydrophobicity and inhibitory activity of the nanoparticles, we plotted the inhibitory activity of each nanoparticle hybrid as a function of the amino acid hydrophobicity.[22] As shown in Figure 6F,G, we found that the inhibition of NF-κB and IRF activation was related to the hydrophobicity of the mutated amino acids. The more hydrophobic the amino acid, the stronger the inhibition. However, this trend did not hold if the amino acid bears an aromatic ring structure (*e.g.*, F, W and Y), as they all exhibited stronger inhibition activity than those having similar hydrophobicity but lacking the aromatic structure. Their inhibitory activity had the following rank order: phenylalanine (F) ≈ tryptophan (W) > tyrosine (Y). The hydrophilic amino acids, serine (S) and threonine (T), and the amino acids with low hydrophobicity such as alanine (A), had little impact on TLR4 signaling. This finding further supported our central hypothesis that the amino acid chemistry on the gold nanoparticles plays

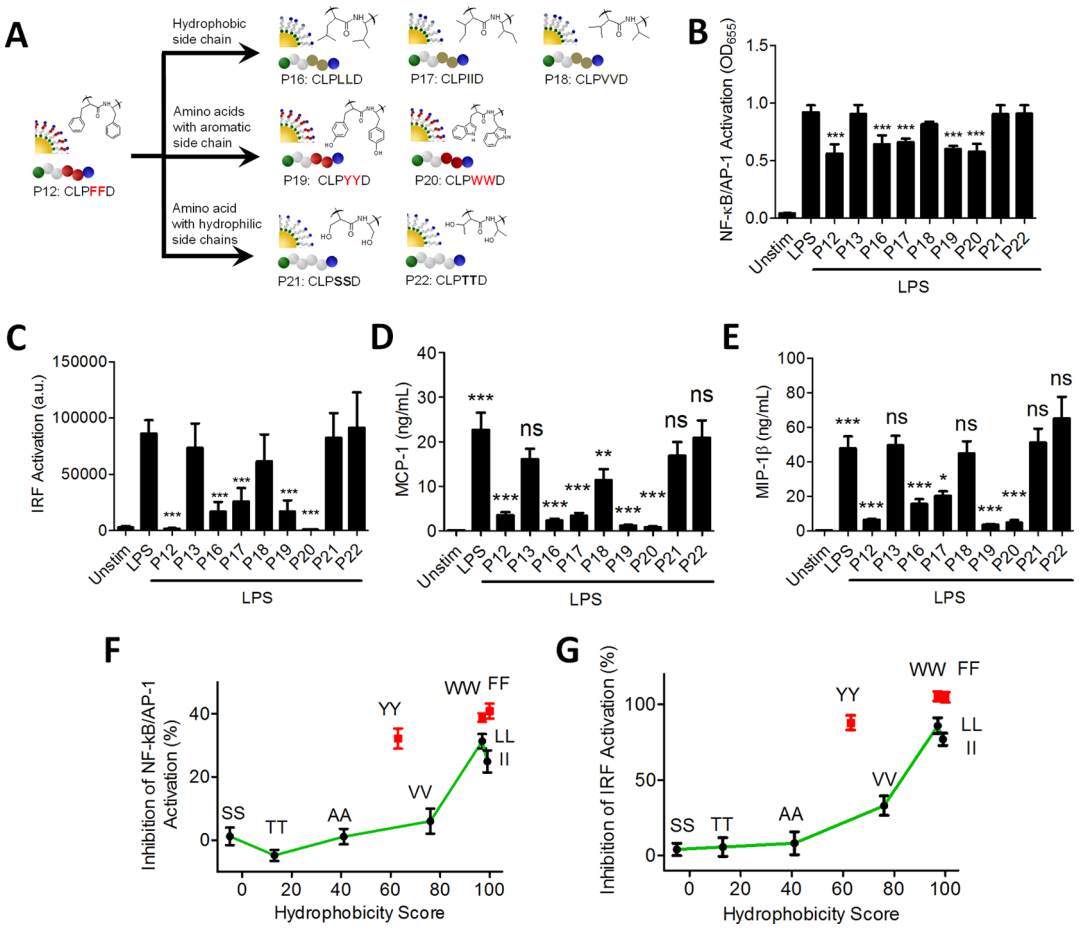


**Figure 6. Effect of amino acid hydrophobicity and structure on the TLR4 inhibitory activity of the peptide-GNP hybrids. (A) A scheme showing the mutation of phenylalanine (F) in P12 to hydrophobic amino acids leucine (L, P16), isoleucine (I, P17) and valine (V, P18), aromatic amino acids tyrosine (Y, P19) and tryptophan (W, P20), or hydrophilic amino acids serine (S, P21) and threonine (T, P22). (B,C) Inhibitory activity of the mutated hybrids on the LPS induced NF-$\kappa$B/AP-1 (B) and IRF (C) activation. (D,E) Effect of mutated hybrids on the LPS induced MCP-1 (D) and MIP-1$\beta$ (E) production on THP1-XBlue cell-derived macrophages. (F,G) The plot of percentage inhibition of NF-$\kappa$B/AP-1 activation (F) and IRF activation (G) as a function of amino acid hydrophobicity score. Nanoparticle concentration = 100 nM, LPS = 10 ng/mL. ns: not significant, *$p < 0.05$, **$p < 0.01$, ***$p < 0.001$ *vs* LPS, $n = 4$.**

a pivotal role in immune modulation. More importantly, it suggested that we can tailor the choice of amino acids displayed on gold nanoparticles to intentionally modulate targeted aspects of the human innate immune response.

**Inhibitory Specificity of P12 on TLR Signaling.** As TLRs share common machinery in their signaling transduction pathways, it is important to know whether nanoparticles specifically block TLR4 signaling or modulate multiple TLR signaling pathways. To address this question, we characterized the activity of P12 on TLRs 2, 3, and 5 signaling using reporter cells. We found that P12 was capable of suppressing the activation of TLRs 2, 3, and 5 stimulated by their specific ligands (Figure 7). Specifically, P12 inhibited the activation of NF-$\kappa$B induced by Pam3CSK4 (TLR2 ligand), poly I:C (TLR3 ligand) and flagellin (TLR5 ligand). P12 also inhibited the IRF activation stimulated by poly I:C. These observations suggested that the inhibitory activity of P12 is not specific to TLR4 signaling, and that P12 could potentially serve as a generic inhibitor for multiple TLR pathways. Interestingly, we found that P12 did not significantly alter interleukin-1 receptor (IL-1R) signaling elicited by either IL-1$\alpha$ or IL-1$\beta$ stimulation (Figure S3). This indicates the specificity of P12 on certain types of membrane receptor signaling pathways (*e.g.*, TLRs) rather than global nonspecific suppression of inflammatory responsiveness.

***In Vivo* Activity of the Lead Nanoparticle Hybrid P12.** To further translate this novel discovery into a potential clinical therapy, we evaluated the anti-inflammatory activity of P12 in a murine model of acute systemic inflammation triggered by LPS. We found that pretreatment of P12, but not P13, significantly reduced levels of cytokines, IL-6 and TNF-$\alpha$, in mouse serum following LPS challenge (Supporting Information Figure S4). This observation indicates that P12 can maintain its anti-inflammatory activity *in vivo* and alleviate acute systemic inflammation induced by LPS. This encouraging *in vivo* data suggests that these

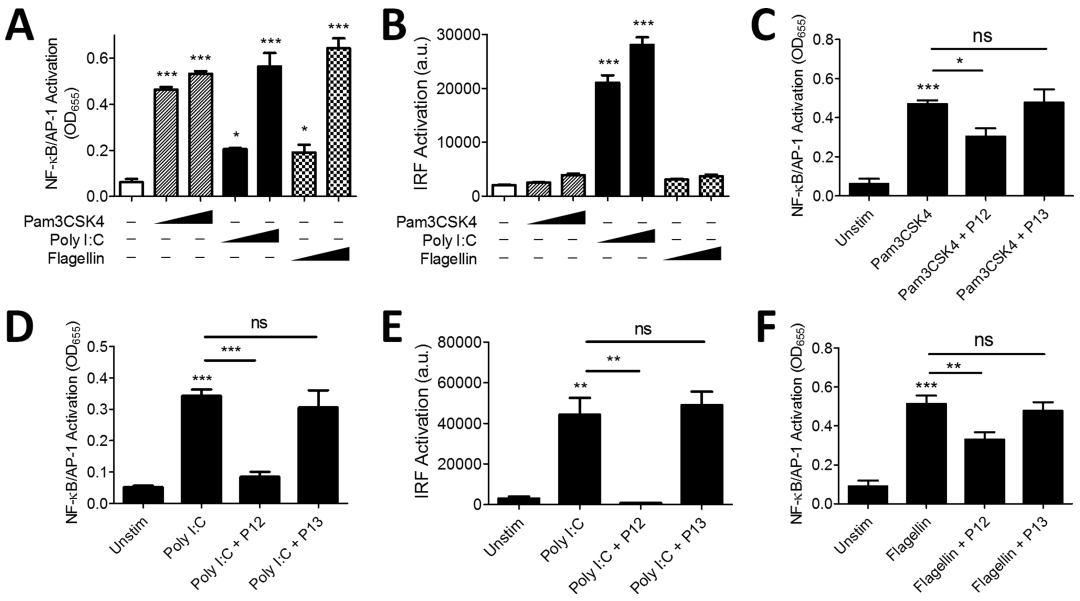


**Figure 7. Effects of P12 and P13 on signaling through other TLRs. (A,B) Activation of NF-$\kappa$B (A) and IRF (B) stimulated by ligands of TLR2 (PAM3CSK4, 1, and 10 ng/mL), TLR3 (poly I:C, 10 and 50 $\mu$g/mL) and TLR5 (flagellin, 10 and 100 ng/mL). (C) Inhibition of NF-$\kappa$B activation by P12 following PAM3CSK4 (1 ng/mL) stimulation. (D,E) Suppression of both NF-$\kappa$B (D) and IRF (E) activation by P12 following poly I:C (50 $\mu$g/mL) stimulation. (F) Reduction of NF-$\kappa$B activation by P12 following flagellin (100 ng/mL) stimulation. *$p < 0.05$, **$p < 0.01$ and ***$p < 0.001$ *vs* unstim unless otherwise indicated, $n = 3-4$.**

anti-inflammatory nanoparticle hybrids could potentially serve as a novel nanotherapy for inflammatory diseases.

## DISCUSSION

The innate immune system and TLR signaling play a vital role in protection from infections. However, TLR signaling is a "double-edged sword" as vigorous innate immune responses can also be harmful, contributing to a variety of human diseases.[4,23,24] Current immunomodulatory interventions to control TLR-mediated pathological inflammation largely rely on global immunosuppressive drugs, particularly corticosteroids, which are often accompanied by significant side-effects. While TLRs have emerged as attractive targets for drug development, there are currently very few compounds available to inhibit TLR signaling. Our study, through screening a nanoparticle library and modulating nanoparticle surface chemistry, has identified a new class of anti-inflammatory reagents. Specifically, we have identified nanoparticles which can inhibit TLR-mediated immune responses in a highly tunable manner in *in vitro* cell culture systems, including primary human mononuclear cells. The identified lead nanoparticles also showed efficacy in an *in vivo* animal model.

Our experimental dissection of molecular structure/chemistry-function relationships revealed that specific peptide coatings on gold nanoparticles can modulate specific aspects of TLR signaling. In particular, as exemplified with TLR4 signaling, the hydrophobicity and aromatic structure of the amino acids were two key factors contributing to the inhibition of TLR4-mediated immune responsiveness: the inhibitory activity of nanoparticles increased with increasing amino acid hydrophobicity; amino acids with aromatic structures had a stronger inhibitory activity than the ones with similar hydrophobicity but lacking the aromatic structure (Figure 6). These findings indicate that by carefully selecting the amino acids displayed on nanoparticles it is possible to tune the degree of inhibition of TLR signaling. To our knowledge, this is the first report to describe differences in the inhibitory capacity of nanoparticles based on their surface-displayed amino acids, and the first to illuminate the relationship between nanoparticle surface chemistry and TLR inhibitory activity. This suggests our approach may represent an entirely new class of immune modulators with significant potential for translation into clinical use.

Our finding of amino acid-dependent inhibition of TLR4 signaling is somewhat reminiscent of an immune evasion strategy used by viruses to inhibit NF-$\kappa$B and IRF3 activation. For example, porcine reproductive and respiratory syndrome virus (PRRSV) inhibits NF-$\kappa$B and IRF3 activation, and the protein region of virus capsid that is critical to this immune suppressive activity is also rich in amino acids with aromatic ring structures.[25]

There are two simple routes to introduce hydrophobic and/or aromatic amino acids into the gold nanoparticle hybrid system. One is to use a binary mixture of peptide ligands with one of the two peptides ending in a hydrophobic/aromatic amino acid (Figure 1A). The advantage of this approach is that the surface properties can be finely controlled by changing the peptide ratios in the mixture. However, this approach is limited

by the potential instability of the nanoparticles due to the addition of the second peptide. For example, nanoparticle hybrids are known to become physiologically unstable when peptides ending in tryptophan or phenylalanine represent more than 10% of the mix.[20] The second route is to introduce the hydrophobic and/or aromatic amino acids into the spacing region of the peptide (Figures 5A and 6A). Through this method, the physiological stability of the hybrids can be maintained with a single peptide coating, while more hydrophobic or aromatic amino acids can be displayed on the nanoparticles. The immunomodulatory activity of the hybrids can be further fine-tuned by altering the numbers and position of the hydrophobic amino acids in the spacer region (Figure 5 and Supporting Information Figure S2).

The mechanism(s) of action of the nanoparticles in suppressing TLR4 signaling remains to be elucidated. Given the similar characteristics of the effective nanoparticles (*i.e.*, hydrophobic or aromatic) and LPS (i,e., hydrophobic), it is reasonable to speculate that the nanoparticles might bind and antagonize LPS, leading to the suppression of TLR4 activation. Although we found that the nanoparticle P12 could bind LPS (Supporting Information Figure S5a,b), this interaction could not be the main inhibitory mechanism for the following reasons. First, P12 can inhibit TLR4 signaling at high LPS concentrations (1 and 10 $\mu$g/mL) at which the binding is saturated (Figure 2A,B). This suggests that the inhibitory activity of P12 is not entirely due to the LPS binding. Second, we found that P12 can also suppress TLR3 signaling without binding with the TLR3 ligand poly I:C (Supporting Information Figure S5c,d). Therefore, based on these data we hypothesize that the nanoparticles may act on intracellular proteins in the common downstream pathways of TLR signaling.

One surprising observation from this study was that hydrophobicity- and aromatic structure-dependent inhibitory effects were most pronounced on the MyD88-independent, IRF3 signaling component of the TLR4 signaling cascade. More potent inhibition of IRF3 activation was observed in the reporter cell assays (Figures 1, 2 and 5, 6) and immunoblots (Figure 3). This trend was also reflected in cytokine measurements. The IRF3-associated chemokines, such as MIP-1$\beta$, were dramatically suppressed, while the MyD88-dependent cytokines, such as IL-6 and IL-8, were less affected by P12 treatment (Figure 4).[26,27] These data are consistent with the observation that TLR4 activates these two signaling pathways from distinct subcellular compartments.[28] The MyD88-dependent pathway is induced from the plasma membrane, whereas the MyD88-independent/IRF3-dependent pathway is triggered from signals originating in the endosome. We have observed that nanoparticle hybrid P12 is internalized into bone marrow-derived dendritic cells and THP-1 cell-derived macrophages generating a punctate pattern (Supporting Information Figure S6),[21] suggesting an endosomal/lysosomal localization of P12. Upon internalization, it is possible that the hydrophobic or aromatic amino acids on P12 may interact with endosomal/lysosomal proteins and interfere the downstream signaling events, preferentially inhibiting the MyD88-independent pathway of TLR4 signaling (*i.e.*, IRF3 activation). Indeed, gold nanoparticles have been found to inhibit TLR9 signaling by interacting with the lysosomal protein, high-mobility group box-1 (HMGB1), and possibly other endosomal/lysosomal proteins.[29] Targeted future experiments are required to define the inhibitory mechanism(s) of action.

## CONCLUSIONS

We have described the discovery of a unique class of nanoparticle hybrids that can potently inhibit TLR-mediated signaling and immune activation. Through screening and evaluating a library of physiologically stable peptide-gold nanoparticle hybrids (with tunable surface chemistry *via* different peptide ligands), we identified a specific hybrid, P12, that potently inhibits both TLR4-triggered NF-$\kappa$B and IRF3 activation, and the secretion of a variety of pro-inflammatory cytokines, including MCP-1, MIP-1$\beta$, and GRO-$\alpha$. The hybrid also suppressed signaling through TLRs 2, 3, and 5. The hydrophobicity and aromatic ring structure of amino acids displayed on the gold nanoparticles were found to play a critical role in this inhibitory activity. By thoughtful selection of the amino acids displayed on nanoparticles, a tunable degree of inhibition of TLR signaling can be achieved. This study defines a new design principle to guide the future development of nanoparticle-based TLR signaling modulators and identifies a novel class of anti-inflammatory therapeutics.

## METHODS

**Gold Nanoparticle Synthesis.** Gold nanoparticles (GNPs) were synthesized according to a modified procedure from the literature.[30] Sodium citrate (2 mL, 38.8 mM, Sigma-Aldrich) was added to the boiling $HAuCl_4$ solution (20 mL, 1.0 mM, Sigma-Aldrich), and the mixture was boiled for 10 min while stirring. The synthesized GNP solution was cooled down for 15 min while stirring and stored at room temperature. The resulting GNPs have a mean size of 13 nm diameter as determined by Hitachi H-7000 electron microscope (Tokyo, Japan) at an accelerating voltage of 70 kV. Before use, the GNP concentration was adjusted to 11 nM, according to its UV–vis absorption spectrum with an extinction coefficient of $2.6 \times 10^8$ $M^{-1}$ $cm^{-1}$ in pure water.

**Preparation of Peptide-GNP Hybrids.** The fabrication of peptide-GNP hybrids was conducted following our published protocol.[20,21] All peptides were synthesized by CanPeptide Inc. (Montreal, Canada) with a purity of >95% and C-terminal protected by amidation. Peptides were dissolved in endotoxin free, ultrapure water as a stock solution of 1 mM. The hybrids

were prepared by mixing one volume of peptide stock solution with ten volume of the synthesized 13 nm GNP solution (final concentration of GNPs is ~11 nM). For the hybrids made of binary peptide ligands, a procedure described in our previous publications was followed.[20,21] Briefly, two different peptide ligands at a volume ratio of 1:19 or 1:9 were mixed with GNPs to provide a total peptide-to-GNP volume ratio of 1:10; thus, the total peptide concentration (100 $\mu$M) remained the same across all formulations. The resulting peptide-GNP hybrids were gently shaken overnight in the dark. All the peptide-GNP hybrids were filtered through a syringe filter (0.22 $\mu$m, Milipore, Billerica, MA, USA). To remove free peptide ligands, the hybrid solutions were centrifuged at 14 000 rpm at 4 °C for 30 min and washed with sterile phosphate buffered saline (PBS) three times. All the hybrids were found to be stable in 150 mM NaCl solution or PBS (*i.e.*, with no solution color change by visualization and UV−vis absorption spectrum).

**Reporter Cells Assay for the Analysis of NF-$\kappa$B/AP-1 and IRF Activation.** THP1-XBlue and THP1-Dual cells were purchased from InvivoGen (San Diego, CA, USA). The reporter cells were cultured as recommended by the supplier using standard protocols. THP1-XBlue cells were cultured in complete RPMI with the addition of Zeocin (100 $\mu$g/mL) to select for cells expressing the SEAP and NF-$\kappa$B/AP-1 reporter. THP1-Dual cells were cultured in complete RPMI with selective antibiotics, Zeocin (100 $\mu$g/mL, InvivoGen) and blasticidin (10 $\mu$g/mL, InvivoGen).

THP-1 reporter cells were differentiated into a macrophage-like phenotype using 50 ng/mL of phorbol 12-myristate 13-acetate (PMA) (Sigma-Aldrich) for 24 h at a density of $1 \times 10^5$ cells/well in 100 $\mu$L in a 96-well plate. Cells were washed with PBS and allowed to rest for 2 days prior to GNP-hybrid treatment and stimulation. Cells were then treated with LPS (1 ng/mL to 10 $\mu$g/mL) in the presence or absence of various hybrids (100 nM) for 24 h or as otherwise stated in the text. Culture media from THP-1 reporter cells was collected and centrifuged at 14 000 rpm at 4 °C for 30 min.

To measure NF-$\kappa$B/AP-1 activation, the supernatants (20 $\mu$L) from THP1-XBlue cells were then incubated with QUANTI-Blue solution (180 $\mu$L) in a 96-well flat-bottom plate at 37 °C for 1−2 h to allow color development. The color change of the substrate solution corresponds to the activation of NF-$\kappa$B/AP-1, which was quantified by optical density ($\lambda$ = 655 nm) measurement using a SpectraMax 384 Plus plate reader (Molecular Devices, Sunnyvale, CA, USA). For the analysis of IRF activation, the supernatants (10 $\mu$L) from THP1-Dual cells were added into a 96-well white plate (flat-bottom) and the luciferase activities were measured using a luminometer (TECAN, Weymouth, U.K.) by autoinjection of QUANTI-Luc assay solution (50 $\mu$L per well).

**PBMCs Isolation.** PBMCs were isolated from peripheral blood of healthy volunteers at Child & Family Research Institute using density gradient centrifugation on Ficoll-Paque Plus (GE Healthcare). The protocol was approved by the University of British Columbia Clinical Research Ethics Board. The cells were then washed twice with PBS and resuspended in complete RPMI. PBMCs were plated in 24-well plates at a density of $5 \times 10^5$ cells/well in 0.5 mL of medium and rested for 1 h. Cells were further stimulated by LPS with the presence and absence of GNP-hybrids.

**Immunoblotting.** THP-1 cells were seeded in 12-well plates (at a density of $2 \times 10^6$ cells/well), differentiated into a macrophage-like phenotype using 100 ng/mL PMA for 72 h. Cells were washed with PBS and allowed to rest for 3 days prior to hybrid treatment and stimulation. Cells were then treated with LPS in the presence or absence of various GNP hybrids (100 nM). Cells were lysed in RIPA buffer supplemented with Halt protease and phosphatase inhibitor cocktail (Thermo Scientific). Protein concentrations were determined by Bradford assay (Thermo Scientific). Lysates were resolved by electrophoreses on 10% SDS-polyacrylamide gels and transferred onto PVDF membranes (Millipore). Blots were blocked with 5% bovine serum albumin in tris-buffered saline (G Biosciences) containing 0.1% TWEEN 20 (Calbiochem) for 1 h at room temperature. The blots were then stained with primary antibodies against p-p65 (Cell Signaling), IkBα (Cell Signaling), p-IRF3 (Cell Signaling), or $\beta$-actin (Cell Signaling) overnight at 4 °C. Another antibody against p-IRF3 (Abcam) together with an antibody against total-IRF3 (Santa Cruz) were employed to verify the specific band for p-IRF3 (indicated by an arrow in Figure 3). Blots were subsequently washed three times with tris-buffered saline containing 0.1% TWEEN 20 and stained with fluorescently labeled secondary antibodies, IRDyeH 680 or 800CW (LI-COR Biosciences) for 1 h. Blots were imaged and quantified on a LI-COR Odyssey infrared imaging system (LI-COR Biosciences).

**Cytokine Analysis.** THP-1 cells were differentiated into a macrophage-like cells using 100 ng/mL PMA for 72 h at a density of $5 \times 10^5$ cells/well in a 24-well plate (0.5 mL/well). Cells were washed with PBS and allowed to rest for 3 days prior to treatment. Cells were then treated with LPS in the presence or absence of various hybrids (100 nM) for 4 and 24 h. Culture media were centrifuged at 14 000 rpm at 4 °C for 30 min. Supernatants were collected and stored at −80 °C. Cytokines released into supernatants were quantified by Luminex-based Procarta custom 23-plex assay (eBioscience, San Diego, CA) and further validated using human ELISA Ready-Set Go kits (eBioscience), following the manufacturer's protocol.

For the Luminex assay, the supernatants were thawed on ice and centrifuged at 500*g* for 5 min. Supernatants were decanted and diluted 1:1 in RPMI, dispensed on a 96 well assay plate and incubated on a shaker at 700 rpm for 2 h and then overnight at 4° with magnetic beads coated with analyte specific antibodies. A biotinylated secondary antibody was added and incubated on the shaker for 30 min. Streptavidin conjugated phycoerythrin was added and incubated on the shaker at room temperature for an additional 30 min. Beads were washed twice with buffer between steps and beads were resuspended in reading buffer before aquisition. Assays were read using Luminex 200 total system running MasterPlex (MiraiBio) software. Cytokines/chemokines quantified in the assay included: GM-CSF (granulocyte macrophage colony-stimulating factor), IL-10 (interleukin 10), IFN-α2 (interferon alpha-2), IL-1$\beta$ (interleukin 1-beta), TNF-α (Tumor necrosis factor-alpha), IL-23 (interleukin-23), IL-12p70 (interleukin 12 p70 subunit), TNF-$\beta$ (tumor necrosis factor-beta), IL-6 (interleukin-6), IL-1RA (interleukin 1 receptor agonist), IL-12p40 (interleukin 12 p40 subunit), IFN-$\gamma$ (interferon gamma), IL-9 (interleukin 9), IP-10 (interferon gamma-induced protein 10/CXCL10), MIP-1$\beta$ (macrophage inflammatory protein 1-beta/CCL4), GRO-α (chemokine ligand-1/CXCL1), MCP-1 (chemokine ligand-2/CCL2), ENA78 (chemokine ligand-5/CXCL5), MCP-3 (chemokine ligand 7/CCL7), M-CSF (macrophage colony stimulating factor), IL-8 (interleukin 8), and MIG (chemokine ligand-9/CXCL9). Standard curves were prepared from premixed standards provided by the manufacturer. Mean fluorescence intensity of the samples was interpolated to analyte quantity using five parameter logistical fit.

**Statistical Analysis.** Data were presented as mean ± standard error of the mean (SEM). Statistical significance was assessed by performing one or two-way ANOVA and the Bonferroni post-test, as applicable. Analyses were performed by using Prism 5 software (GraphPad). A *p*-value of <0.05 was considered significant.

*Conflict of Interest:* The authors declare no competing financial interest.

*Acknowledgment.* The financial support for this project was provided by grants to S.E.T. from Cystic Fibrosis Canada (CF Canada), Natural Sciences and Engineering Research Council of Canada (NSERC) and the Crohn's and Colitis Foundation of Canada (CCFC), and by grants to M.L. from Canadian Institute of Health Science (CIHR). S.E.T. holds the Aubrey J. Tingle Professorship in Pediatric Immunology and is a clinical scholar of the Michael Smith Foundation for Health Research. S.Y.F. is supported by a postdoctoral fellowship from the Child & Family Research Institute. T.R.K. is supported in part by a Career Award in the Biomedical Sciences from the Burroughs Welcome Fund and a Michael Smith Foundation for Health Research Career Investigator Award.

*Supporting Information Available:* Additional figures describing cytokine production analysis at 4 h, the effect of the

number and location of phenylalanine on cytokine analysis, the inhibitory specificity of P12, the *in vivo* efficacy of nanoparticles in murine model of acute systemic inflammation, nanoparticle and TLR ligand binding analysis, and the confocal microscopic imaging of nanoparticles internalized into cells. The Supporting Information is available free of charge on the ACS Publications website at DOI: 10.1021/nn505634h.

## REFERENCES AND NOTES


1. Lemaitre, B.; Nicolas, E.; Michaut, L.; Reichhart, J. M.; Hoffmann, J. A. The Dorsoventral Regulatory Gene Cassette Spatzle/Toll/Cactus Controls the Potent Antifungal Response in Drosophila Adults. *Cell* **1996**, *86*, 973–983.
2. Turvey, S. E.; Durandy, A.; Fischer, A.; Fung, S. Y.; Geha, R. S.; Gewies, A.; Giese, T.; Greil, J.; Keller, B.; McKinnon, M. L.; *et al.* The CARD11-BCL10-MALT1 (CBM) Signalosome Complex: Stepping into the Limelight of Human Primary Immunodeficiency. *J. Allergy Clin. Immunol.* **2014**, *134*, 276–284.
3. Turvey, S. E.; Broide, D. H. Innate Immunity. *J. Allergy Clin. Immunol.* **2010**, *125*, S24–32.
4. Honda, K.; Taniguchi, T. IRFs: Master Regulators of Signaling by Toll-like Receptors and Cytosolic Pattern-Recognition Receptors. *Nat. Rev. Immunol.* **2006**, *6*, 644–658.
5. Wittebole, X.; Castanares-Zapatero, D.; Laterre, P. F. Toll-like Receptor 4 Modulation as a Strategy to Treat Sepsis. *Mediators Inflammation* **2010**, *2010*, 568396.
6. Leon, C. G.; Tory, R.; Jia, J.; Sivak, O.; Wasan, K. M. Discovery and Development of Toll-like Receptor 4 (TLR4) Antagonists: a New Paradigm for Treating Sepsis and Other Diseases. *Pharm. Res.* **2008**, *25*, 1751–1761.
7. de Souza, F. N.; Sanchez, E. M. R.; Henemmann, M. B.; Gidlund, M. A.; Reis, L. D. C.; Blagitz, M. G.; Libera, A. M. M. P. D.; Cerqueira, M. M. O. P. The Innate Immunity in Bovine Mastitis: the Role of Pattern-Recognition Receptors. *Am. J. Immunol.* **2012**, *8*, 166–178.
8. Wellnitz, O.; Bruckmaier, R. M. The Innate Immune Response of the Bovine Mammary Gland to Bacterial Infection. *Vet. J.* **2012**, *192*, 148–152.
9. Aline, F.; Brand, D.; Pierre, J.; Roingeard, P.; Severine, M.; Verrier, B.; Dimier-Poisson, I. Dendritic Cells Loaded With HIV-1 P24 Proteins Adsorbed on Surfactant-Free Anionic PLA Nanoparticles Induce Enhanced Cellular Immune Responses Against HIV-1 after Vaccination. *Vaccine* **2009**, *27*, 5284–5291.
10. Patterson, D. P.; Rynda-Apple, A.; Harmsen, A. L.; Harmsen, A. G.; Douglas, T. Biomimetic Antigenic Nanoparticles Elicit Controlled Protective Immune Response to Influenza. *ACS Nano* **2013**, *7*, 3036–3044.
11. Shaunak, S.; Thomas, S.; Gianasi, E.; Godwin, A.; Jones, E.; Teo, I.; Mireskandari, K.; Luthert, P.; Duncan, R.; Patterson, S.; *et al.* Polyvalent Dendrimer Glucosamine Conjugates Prevent Scar Tissue Formation. *Nat. Biotechnol.* **2004**, *22*, 977–984.
12. Blohmke, C. J.; Mayer, M. L.; Tang, A. C.; Hirschfeld, A. F.; Fjell, C. D.; Sze, M. A.; Falsafi, R.; Wang, S.; Hsu, K.; Chilvers, M. A.; *et al.* Atypical Activation of the Unfolded Protein Response in Cystic Fibrosis Airway Cells Contributes to P38 MAPK-Mediated Innate Immune Responses. *J. Immunol.* **2012**, *189*, 5467–5475.
13. Hunter, Z.; McCarthy, D. P.; Yap, W. T.; Harp, C. T.; Getts, D. R.; Shea, L. D.; Miller, S. D. A Biodegradable Nanoparticle Platform for the Induction of Antigen-Specific Immune Tolerance for Treatmentof Autoimmune Disease. *ACS Nano* **2014**, *8*, 2148–2160.
14. Dernedde, J.; Rausch, A.; Weinhart, M.; Enders, S.; Tauber, R.; Licha, K.; Schirner, M.; Zugel, U.; von, B. A.; Haag, R. Dendritic Polyglycerol Sulfates as Multivalent Inhibitors of Inflammation. *Proc. Natl. Acad. Sci. U. S. A* **2010**, *107*, 19679–19684.
15. Bhattacharjee, H.; Balabathula, P.; Wood, G. C. Targeted Nanoparticulate Drug-Delivery Systems for Treatment of Solid Tumors: a Review. *Ther. Delivery* **2010**, *1*, 713–734.
16. Laroui, H.; Sitaraman, S. V.; Merlin, D. Gastrointestinal Delivery of Anti-Inflammatory Nanoparticles. *Methods Enzymol.* **2012**, *509*, 101–125.
17. von, M. G.; Park, J. H.; Lin, K. Y.; Singh, N.; Schwoppe, C.; Mesters, R.; Berdel, W. E.; Ruoslahti, E.; Sailor, M. J.; Bhatia, S. N. Nanoparticles That Communicate *in vivo* to Amplify Tumour Targeting. *Nat. Mater.* **2011**, *10*, 545–552.
18. Chellat, F.; Merhi, Y.; Moreau, A.; Yahia, L. H. Therapeutic Potential of Nanoparticulate Systems for Macrophage Targeting. *Biomaterials* **2005**, *26*, 7260–7275.
19. Laroui, H.; Viennois, E.; Xiao, B.; Canup, B. S.; Geem, D.; Denning, T. L.; Merlin, D. Fab'-Bearing SiRNA TNFalpha-Loaded Nanoparticles Targeted to Colonic Macrophages Offer an Effective Therapy for Experimental Colitis. *J. Controlled Release* **2014**, *186*, 41–53.
20. Yang, H.; Fung, S.-Y.; Liu, M. Programming the Cellular Uptake of Physiologically Stable Peptide−Gold Nanoparticle Hybrids with Single Amino Acids. *Angew. Chem., Int. Ed.* **2011**, *50*, 9643–9646.
21. Yang, H.; Zhou, Y.; Fung, S. Y.; Wu, L.; Tsai, K.; Tan, R.; Stuart, T.; Machuca, T.; de Perrot, M.; Waddell, T.; *et al.* Amino Acid Structure Determines the Immune Responses Generated by Peptide-Gold Nanoparticle Hybrids. *Part. Part. Syst. Charact.* **2013**, *30*, 1039–1043.
22. Monera, O. D.; Sereda, T. J.; Zhou, N. E.; Kay, C. M.; Hodges, R. S. Relationship of Sidechain Hydrophobicity and α-Helical Propensity on Stability of the Single-Stranded Amphipathic α-Helix. *J. Protein Sci.* **1995**, *1*, 319–329.
23. Midwood, K. S.; Piccinini, A. M.; Sacre, S. Targeting Toll-like Receptors in Autoimmunity. *Curr. Drug Targets* **2009**, *10*, 1139–1155.
24. Huang, B.; Zhao, J.; Unkeless, J. C.; Feng, Z. H.; Xiong, H. TLR Signaling by Tumor and Immune Cells: a Double-Edged Sword. *Oncogene* **2008**, *27*, 218–224.
25. Song, C.; Krell, P.; Yoo, D. Nonstructural Protein 1alpha Subunit-Based Inhibition of NF-KappaB Activation and Suppression of Interferon-Beta Production by Porcine Reproductive and Respiratory Syndrome Virus. *Virology* **2010**, *407*, 268–280.
26. Andersen, J.; VanScoy, S.; Cheng, T.-F.; Gomez, D.; Reich, N. C. IRF-3-Dependent and Augmented Target Genes during Viral Infection. *Genes Immun.* **2008**, *9*, 168–175.
27. Hui, K. P. Y.; Lee, SM. Y.; Cheung, C.; Ng, I. H. Y.; Poon, L. L. M.; Guan, Y.; Ip, N. Y. Y.; Lau, A. S. Y. P. J. S. M. Induction of Proinflammatory Cytokines in Primary Human Macrophages by Influenza A Virus (H5N1) Is Selectively Regulated by IFN Regulatory Factor 3 and P38 MAPK. *J. Immunol.* **2009**, *182*, 1088–1098.
28. Kagan, J. C.; Su, T.; Horng, T.; Chow, A.; Akira, S.; Medzhitov, R. TRAM Couples Endocytosis of Toll-like Receptor 4 to the Induction of Interferon-β. *Nat. Immunol.* **2008**, *9*, 361–368.
29. Tsai, C. Y.; Lu, S. L.; Hu, C. W.; Yeh, C. S.; Lee, G. B.; Lei, H. Y. Size-Dependent Attenuation of TLR9 Signaling by Gold Nanoparticles in Macrophages. *J. Immunol.* **2012**, *188*, 68–76.
30. Storhoff, J. J.; Elghanian, R.; Mucic, R. C.; Mirkin, C. A.; Letsinger, R. L. One-Pot Colorimetric Differentiation of Polynucleotides with Single Base Imperfections Using Gold Nanoparticle Probes. *J. Am. Chem. Soc.* **1998**, *120*, 1959–1964.